

Mixed-kinematic body sideslip angle estimator for high performance cars

Olga Galluppi¹, Matteo Corno¹ and Sergio M. Savaresi¹

Abstract—Body sideslip angle estimation is a well-known issue in the automotive field. Many vehicle dynamic control systems are based on the control or monitoring of the sideslip angle. Unfortunately, measurement of this quantity requires expensive instrumentation that commercial cars can not be equipped with. This paper further develops the so-called hybrid dynamic-kinematic approach to the problem providing an automated tuning approach. A state observer merges a kinematic model with a lateral dynamic one, so that they can compensate each other shortcomings. The resulting estimator depends on a number of parameters whose manual tuning require expertise. The paper proposes a grey-box approach for the tuning of the algorithm. The optimization-based approach requires only standard track tests and no special vehicle characterization. The approach is validated on a large experimental dataset from a high performance car.

I. INTRODUCTION

In the automotive field, stability control is one of the major issues regarding passenger's safety and Electronic Stability Control (ESC) is nowadays standard on commercial cars [3]. One of its primary objective is to keep the body sideslip angle (the angle formed by the vehicle's longitudinal axis and its velocity vector on the horizontal plane) as close as possible to zero [2]. Unfortunately, this quantity is not easily measurable (no low-cost direct instrumentation exists) and needs to be estimated on-line through commonly available signals. Over the year, industry and academic have dedicated a great effort to this topic, incrementally improving the accuracy and reliability of the estimation.

The relevant literature can be divided in two general categories: black box models and physics-based models. Black box models include all kind of nonlinear functions that are optimized to match experimental data, such as neural networks [4] and data-driven approaches [5]. Physics-based models can be further divided in two sub-categories: kinematic models and dynamic models. Kinematic approaches [8] rely on a simple vehicle model description that correlates basic kinematic quantities. As a result, these methods do not depend on the specific vehicle or tyre friction parameters, but suffer from the problem of straight-driving drifting [7]. Oppositely, dynamic approaches include knowledge of the vehicle parameters, especially different types of tyre-road contact forces modelization, in order to describe the vehicle's lateral dynamics. Those models are vehicle and road dependent and usually require specific experimental tests and knowledge of the system to be tuned.

A third approach is the hybrid approach where both the kinematic and dynamic information is employed [6]-[9]. These approaches mix a general kinematic approach, which does not include any vehicle-dependent parameters, with a very simple lateral dynamic model of the vehicle.

The algorithm discussed and developed in this work is inspired by [9] in its mixed nature, and improves the state-of-the-art approach under three aspects:

- The longitudinal velocity estimation is improved by using the information coming from the four wheels encoder and the longitudinal accelerometer.
- A general tuning procedure for all the observer's parameters is discussed, which does not require any specific dynamical test or knowledge, as long as having an experimental dataset (including sideslip measure) that would describe the vehicle's lateral attitude enough. The observer modular architecture permits the separate definition of the different layers of the observer, being extremely adaptable.
- The observer is validated on a high performance sport car. The paper provides a thorough analysis of the results during a handful of different challenging maneuvers.

On the other hand, differently from [9] this work does not consider the tyre friction estimation.

The paper is organized as follows: the general observer architecture and all its modules are presented in Section II. Section III discusses the general tuning procedure for all the observer's parameters, and Section IV presents the experimental results.

II. OBSERVER DESIGN

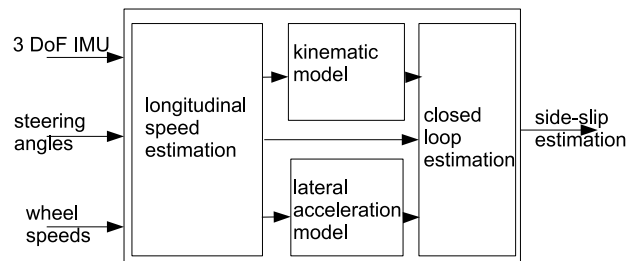


Fig. 1: Sideslip observer general modular architecture.

The observer's modular architecture is depicted in Figure 1: the kinematic baseline model is used in output feedback including a longitudinal speed estimate and a lateral acceleration dynamic model.

¹ Authors are with Dipartimento di Elettronica, Informazione e Bioingegneria (DEIB), Politecnico di Milano, Piazza Leonardo Da Vinci, 20133, Milano, Italy. Corresponding author: olga.galluppi@polimi.it

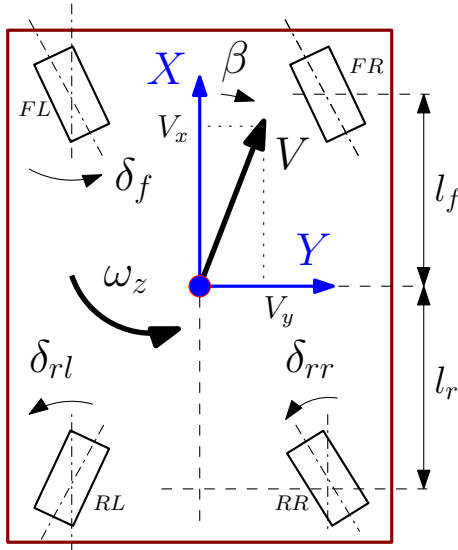


Fig. 2: Vehicle reference system. The general case of a 4-wheel steering (4WS) car is considered: while the front wheels angle δ_f is controlled by the driver through the steering wheel, the two rear wheels are motorized and can be rotated autonomously. l_f, l_r are respectively the vehicle's front and rear wheelbase. FL, FR, RL, RR indicates the four wheels w by $\{\text{Front, Rear}\}\{\text{Left, Right}\}$.

The baseline kinematic vehicle's lateral model [8] is

$$\underbrace{\begin{bmatrix} \dot{V}_x(t) \\ \dot{V}_y(t) \end{bmatrix}}_{\dot{x}(t)} = \underbrace{\begin{bmatrix} 0 & -\omega_z(t) \\ \omega_z(t) & 0 \end{bmatrix}}_{A(t)} \underbrace{\begin{bmatrix} V_x(t) \\ V_y(t) \end{bmatrix}}_{x(t)} + \underbrace{\begin{bmatrix} 1 & 0 \\ 0 & 1 \end{bmatrix}}_B \underbrace{\begin{bmatrix} A_x(t) \\ A_y(t) \end{bmatrix}}_{u(t)} \quad (1)$$

where $V_x(t), V_y(t)$ are respectively the vehicle's body longitudinal and lateral velocity components, $\omega_z(t)$ is the yaw rate and $A_x(t), A_y(t)$ are longitudinal and lateral barycentric accelerations. Yaw rate and acceleration signals are nowadays available from any vehicle's Inertial Measurement Unit (IMU). See Figure 2 for the considered vehicle reference system. The model (1) is a second order linear time-varying dynamical system with state $x(t)$, input $u(t)$ and state matrices $A(t)$ and B . Its time variance is due to the yaw rate dependency of matrix A . This model is fully kinematic and does not contain any vehicle parameter. The vehicle's body sideslip angle $\beta(t)$ is given by

$$\beta(t) = \arctan \frac{V_y(t)}{V_x(t)} \quad (2)$$

and the development of an estimator of state $x(t)$ is equivalent to the estimation of the sideslip angle.

To implement an effective state observer for (1), the proposed strategy is to enrich the state equations with some known output model $\hat{y}(t)$ of quantities $y(t)$ that are measurable and sideslip-related. Similar approaches have been developed in [6],[9]. The feedback is imposed on the following output

$$y(t) = \begin{bmatrix} V_x^m(t) \\ A_y(t) \end{bmatrix}, \quad \hat{y}(t) = \begin{bmatrix} \hat{V}_x(t) \\ \hat{A}_y(t) \end{bmatrix} \quad (3)$$

where $V_x^m(t)$ is the vehicle's *estimated* longitudinal speed, and a state-dependent model law for the second output $\hat{A}_y(t)$ must be defined. Longitudinal speed is not generally available as a measure in a commercial vehicle, but can be estimated using more commonly present signals. The model used for lateral acceleration and the longitudinal velocity estimation are discussed in the following subsections.

The general feedback observer model is then given by

$$\begin{bmatrix} \dot{\hat{V}}_x(t) \\ \dot{\hat{V}}_y(t) \end{bmatrix} = A(t) \begin{bmatrix} \hat{V}_x(t) \\ \hat{V}_y(t) \end{bmatrix} + B \begin{bmatrix} A_x(t) \\ A_y(t) \end{bmatrix} + \underbrace{\begin{bmatrix} k_x & 0 \\ 0 & k_y \end{bmatrix}}_K \underbrace{\begin{bmatrix} V_x^m(t) - \hat{V}_x(t) \\ A_y(t) - \hat{A}_y(t) \end{bmatrix}}_{y(t) - \hat{y}(t)} \quad (4)$$

Remark 1: A standard signal pre-processing module similar to the one described and detailed in [7] should be annexed to the estimator. This includes signals filtering, center of mass transportation, sensor offset estimation and roll compensation.

A. Lateral acceleration model

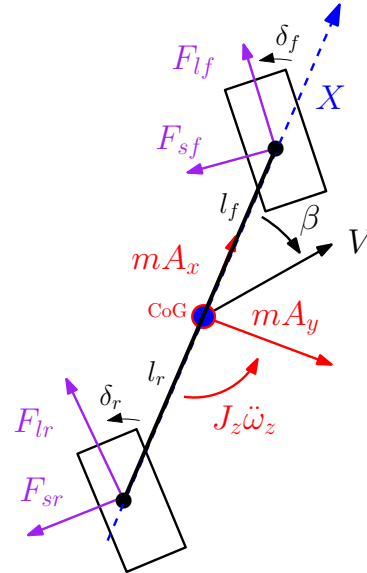


Fig. 3: Bicycle model with road contact forces. m is the vehicle mass and J_z is the vehicle vertical moment of inertia. The rear steering angle $\delta_r = \frac{\delta_{rl} + \delta_{rr}}{2}$ is taken as the mean between left and right.

Providing a model of the vehicle's lateral acceleration which is both effective, simple and whose parameters are easily tuned is not an easy task. In this work, the bicycle model of Figure 3 is employed, with the purpose of having as few vehicle-dependent parameters as possible. This model is widely used in literature and automotive applications [10] and couples the two front and rear wheels together respectively. Being extremely simple, it neglects various effects (such as load transfer, vertical dynamics interaction,...) still being able to capture the major lateral dynamics responses.

Inertial forces (in red in Figure 3) are condensed in the vehicle's Center of Gravity (CoG) and counteract the road contact forces (in purple, partitioned in longitudinal $F_{lf}(t), F_{lr}(t)$ and lateral $F_{sf}(t), F_{sr}(t)$ components).

For the lateral acceleration model $\hat{A}_y(t)$ of this work, longitudinal and lateral dynamics are considered as decoupled, e.g. no longitudinal acceleration action $F_{lf}(t), F_{lr}(t)$ is considered on cornering.

Under the movement decoupling hypothesis, the system's lateral equilibrium resolves into

$$\hat{A}_y(t) = m^{-1}(\hat{F}_{sf}(t) \cos \delta_f(t) + \hat{F}_{sr}(t) \cos \delta_r(t)). \quad (5)$$

where

$$\begin{aligned} \hat{F}_{sf}(t) &= 2 \frac{C_{sf}}{k_f} \tanh(k_f \alpha_f(t)) \\ \hat{F}_{sr}(t) &= 2 \frac{C_{sr}}{k_r} \tanh(k_r \alpha_r(t)) \end{aligned} \quad (6)$$

where C_{sf}, C_{sr} are the well known front and rear cornering stiffness doubled to account for the two wheels [10], parameters which resume tyres lateral performance, and $\alpha_f(t), \alpha_r(t)$ are front and rear mean wheel-slip angles, namely the angle formed by the wheel's velocity vector $V_f(t), V_r(t)$ and its vertical plane (see Figure 4), defined as in Eq. (7).

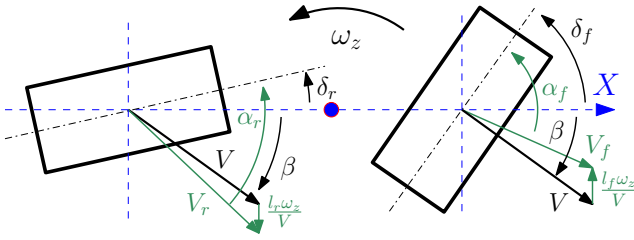


Fig. 4: Wheel slip angles.

$$\begin{aligned} \alpha_f(t) &= \beta(t) + \delta_f(t) - \frac{l_f \omega_z(t)}{V(t)} \\ \alpha_r(t) &= \beta(t) + \delta_r(t) + \frac{l_r \omega_z(t)}{V(t)} \end{aligned} \quad (7)$$

The hyperbolic tangent model of contact forces of Eq. (6), with coefficients k_f, k_r , differently from other contact forces models accounts for saturation of the wheel's lateral load, as the force tends to the value $C_{sf}/k_f, C_{sr}/k_r$ for angles $\alpha_f(t), \alpha_r(t)$ tending toward infinity. In literature, the dependence of the force over the wheel slip angles is usually modeled as linear, thus having a force tending towards infinity with the angle. For angles close to zero, model (6) tends to the linear one. The proposed model offers a good trade-off between the number of parameters and the descriptive power. Guidelines on how to tune the four model parameters C_{sf}, C_{sr}, k_f, k_r are given in Section III.

B. Longitudinal Velocity Estimation

The sideslip angle estimation algorithm (4) assumes the availability of the longitudinal velocity measurement. Such a measurement is not directly available. Instead an estimation

derived from the wheels speed is employed. Wheels velocities provide some information on the longitudinal vehicle speed, but they are not reliable in all conditions as tyres can be subject to large longitudinal slip. This is especially true for sport vehicles and aggressive driving as considered in this work.

The longitudinal velocity estimation algorithms considers the above fact and estimates the longitudinal velocity by merging the four available wheel speeds. The algorithm is summarized in Figure 5. When a wheel generates an acceler-

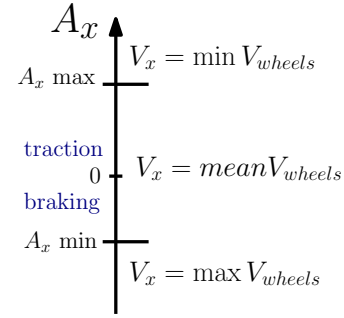


Fig. 5: Longitudinal velocity estimation algorithm.

ating force, the wheel speed is greater than the vehicle speed. Hence, when the vehicle is accelerating, the most reliable measurement, among the four wheel speed measurements, is the lowest one. Viceversa, when a wheel is decelerating the vehicle, its speed is smaller than the vehicle speed, thus on decelerating maneuvers the most reliable measurement for the vehicle speed is the highest wheel speed. Acceleration and deceleration maneuvers are identified through thresholds on the longitudinal acceleration (A_x). When the vehicle is neither accelerating nor braking, the algorithm computes longitudinal velocity estimation as the average of the four wheels.

III. PARAMETERS TUNING

Observer (4) is completely defined by a number of parameters $\mathcal{P} = \{\mathcal{C}, k_x, k_y\}$

- The 4 parameters $\mathcal{C} = \{C_{sf}, C_{sr}, k_f, k_r\}$ define the lateral acceleration model of (5)-(6).
- The static gain k_x fixes the longitudinal feedback over V_x^m and sets the level of reliability of such quantity.
- The gain k_y fixes the lateral feedback.

Tuning the above parameters may not be easy, here an automatic tuning procedure is adopted:

- **step 1:** Identify the dynamical model for lateral acceleration.
- **step 2:** Tune all the parameters to optimize estimation results.

The procedure applies nonlinear optimization through a *gray-box* philosophy fashion. The only requirement is to have a dataset \mathcal{D} of onboard standard measures and sideslip angle measures $\tilde{\beta}(t)$ from the vehicle. The experiments should describe the conditions in which the vehicle is expected to operate.

The first step to be done is to compute the set of parameters \mathcal{C} through the following:

- 1) Isolate data $\tilde{\mathcal{D}} \subset \mathcal{D}$ for which longitudinal acceleration and yaw acceleration $\ddot{\omega}_z(t)$ is low.
- 2) Compute experimental wheel slip angles $\tilde{\alpha}_f(t), \tilde{\alpha}_r(t)$ as in (7) from data $\tilde{\mathcal{D}}$.
- 3) Compute empirical forces $\tilde{F}_{sf}(t), \tilde{F}_{sr}(t)$ from data $\tilde{\mathcal{D}}$ imposing (5) and torques equilibrium on the model of Figure 3, considering zero yaw acceleration.
- 4) Solve the two nonconvex optimization problems

$$\begin{aligned} \{C_{sf}, k_f\} &= \arg \min_{\tilde{C}_{sf}, \tilde{k}_f} \|\tilde{F}_{sf}(t) - \hat{F}_{sf}(\tilde{\alpha}_f(t), \tilde{C}_{sf}, \tilde{k}_f)\|_2^2 \\ \{C_{sr}, k_r\} &= \arg \min_{\tilde{C}_{sr}, \tilde{k}_r} \|\tilde{F}_{sr}(t) - \hat{F}_{sr}(\tilde{\alpha}_r(t), \tilde{C}_{sr}, \tilde{k}_r)\|_2^2 \end{aligned} \quad (8)$$

imposing model (6). Note that the identified parameters would depend on the particular road surface the dataset have been collected on.

The second step of the tuning procedure is then to optimize parameters \mathcal{P} of the observer over sideslip estimation results $\hat{\beta}(t) = \hat{\beta}(t, \mathcal{P})$ through the following cost function J_β :

$$J_\beta(\mathcal{P}) = \left\| \hat{\beta}(t_\beta) - \tilde{\beta}(t_\beta) \right\|_2^2 \quad t_\beta \in \mathcal{B} \subset \mathcal{D} \quad (9)$$

where the set \mathcal{B} represents a subset of time instants t_β of the available dataset \mathcal{D} for which the following conditions apply:

- Longitudinal velocity $V_x(t)$ is higher than a fixed threshold of interest (e.g. $V_x(t_\beta) > 20$ [km/h]),
- The absolute value of measured sideslip $\tilde{\beta}(t)$ is contained in a fixed region of interest (e.g. $2 < |\tilde{\beta}(t_\beta)| < 12$ [deg]).

Out of the considered conditions (i.e. very low speed and/or angles of sideslip very small or very large) sideslip estimation can not be considered a concern for passenger's safety [2][3]: vehicle stability is not an issue for very low speed or very low sideslip angle, and very large sideslip angles should never be reached during normal driving conditions, as the stability controller would surely react before their realization. Also note that restricting the optimization routine over a subset of conditions of interest manages to focus estimation results precision in that region.

The overall tuning is called *grey-box* as the physical-valued parameters \mathcal{C} , obtained through the first step, can be modified from the optimization routine of the second step towards non-strictly physics-based parameters, as to obtain better estimation results.

Remark 2: Wheel load variations are taken into account when tuning the lateral feedback gain k_y : its value defines the relative weight of dynamic and kinematic model, and permits the reaching of their best trade-off through the data-driven optimization routine.

IV. EXPERIMENTAL RESULTS

This section tests the algorithm on a high-performance sport car. Total duration of the experiment is more than

1 hour, for a total of $\approx 850k$ samples (sampling time is 0.005 [s]). The actual sideslip angle is measured with an optical sensor, A_y, A_x, ω_z are from the vehicle's production-grade IMU, and the 4 wheels speed and steering angle come from standard encoders. The experiments have been performed on different handling circuits (over dry surface, mounting both new and worn tyres) and contain extreme driving manoeuvres, that couple high lateral and longitudinal dynamic conditions as shown in the g-g plot of Figure 6.

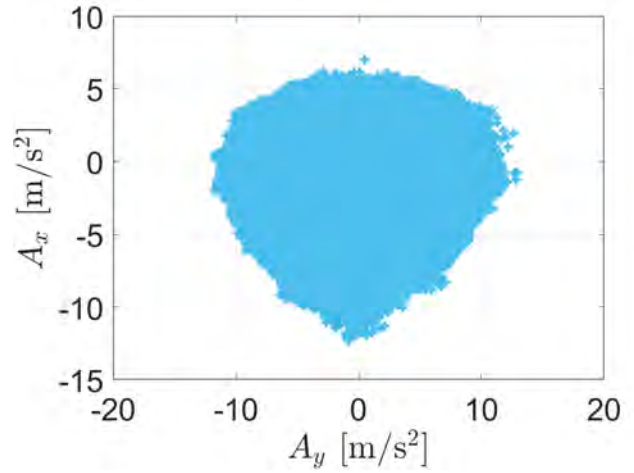


Fig. 6: All data g-g plot.

The results of the first step of the tuning procedure, setting the dynamical model of (6), are shown in Figure 7. Note

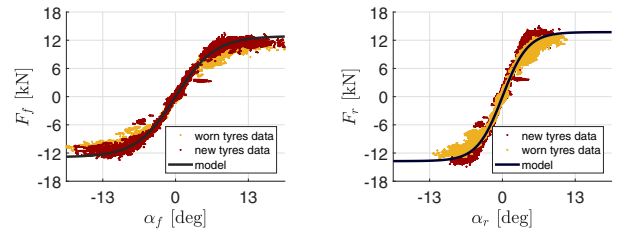


Fig. 7: Identified single track dynamical model (front and rear).

that the proposed models do not perfectly fit the data (and try to average between the two set of tyres). The simplified tyre model does not have enough parameters to perfectly fit the actual tyre characteristics, nevertheless the closed-loop nature of the estimation approach will compensate for this modeling error. A more complex tyre model would ensure a greater accuracy, but it would increase the risk of overfitting and thus reduce robustness.

The estimator parameters are optimized through cost function (9) for speed over 20 [km/h] and absolute sideslip angle values between 2 and 12 [deg]. The following figures show a collection of interesting manoeuvres out of available data. Figure 8 shows two acceleration manoeuvres. During the first acceleration, (seconds [520 – 527]) the vehicle reaches small sideslip angles ($\beta < 5$ deg) while the steer is swepted.

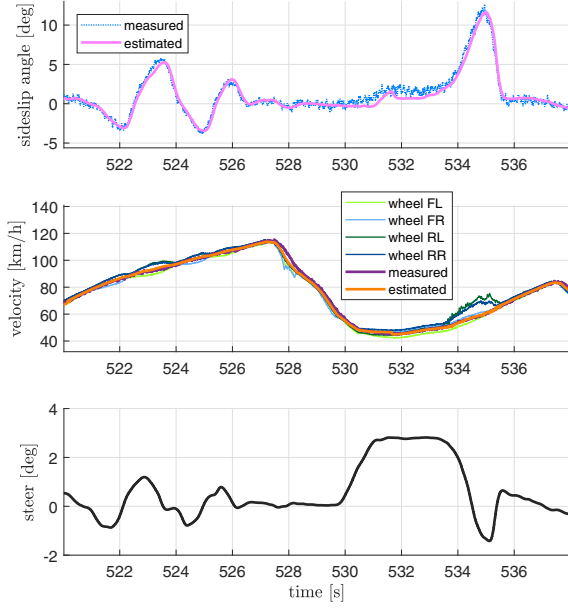


Fig. 8: Validation details.

The algorithm very accurately estimates these small, rapidly varying angles. The interval ([530 – 536]) shows a corner followed by a sharp acceleration. During this maneuver a higher sideslip is reached and the driver introduces a countersteering action. Also in this case the algorithm accurately tracks the sideslip angle. Further note that at second 534, the acceleration is so strong that the rear wheels start slipping. In this context, the longitudinal velocity estimation algorithm is capable of estimating the true vehicle velocity.

The second detailed analysis of Figure 9 better shows the properties of the estimator when the vehicle reaches higher sideslip angles. Recall that at these angles the exploited model is not very accurate. Nevertheless the estimate is still extremely accurate, thanks to the merging of the kinematic and dynamic parts. Further note that the estimate is both statically and dynamically accurate.

Finally, Figure 10 plots a tract of the track where very small side slip angles are maintained for an extended period of time. These conditions, rarely analyzed in the literature, are actually very challenging because the kinematic estimation suffers from drift. The use of the dynamic model alleviates this issue.

Figure 11 summarizes the performance of the proposed algorithm: with 87% of samples having estimation error $e_{\beta}(t) = \hat{\beta}(t) - \beta(t)$ less than 1 [deg].

V. CONCLUSIONS

The paper presents a detailed analysis of a sideslip angle estimation using only standard onboard vehicles measurement. The idea of the algorithm is to merge the kinematic and dynamic information into a single closed loop approach. The resulting method has a number of tuning parameters

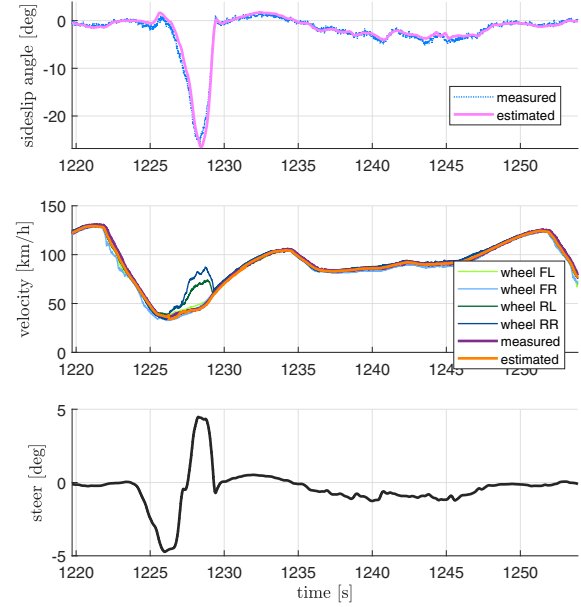


Fig. 9: Validation details.

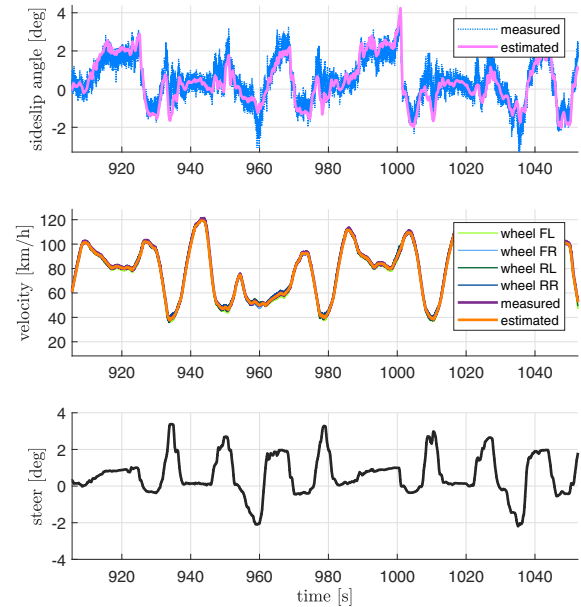


Fig. 10: Validation details.

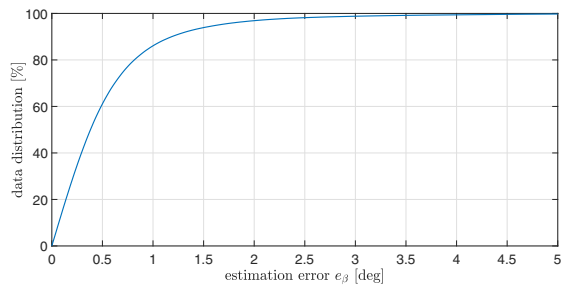


Fig. 11: Estimation error cumulative density function distribution.

whose tuning may be difficult, to solve this issue and make the tuning of the algorithm more efficient a two-step grey box tuning procedure is proposed.

The proposed observer attains excellent estimation results in high performance driving situations. Future research will be devoted to the testing of its robustness with respect to different road surfaces.

REFERENCES

- [1] G. Panzani, M. Corno, M. Tanelli, S. M. Savaresi, A. Fortina, and S. Campo, Control-oriented vehicle attitude estimation with online sensors bias compensation. Proc. of ASME 2009 Dynamic Systems and Control Conference, 2009, pp. 819826.
- [2] E.K. Liebmenn, K. Meder, J. Schuh, and G. Nenninger, Safety and Performance Enhancement: The Bosch Electronic Stability Control (ESP). SAE Technical Paper, 2004.
- [3] S.A. Ferguson, The effectiveness of electronic stability control in reducing real-world crashes: a literature review. Traffic injury prevention, Vol. 8, No. 4, 2007, pp. 329-338.
- [4] H. Sasaki and T. Nishimaki, A side-slip angle estimation using neural network for a wheeled vehicle. SAE Technical Paper, 2000.
- [5] M. Milanese, D. Regruto and A. Fortina, Direct virtual sensor (DVS) design in vehicle sideslip angle estimation. Proc. of the American Control Conference (ACC), 2007, pp. 3654-3658.
- [6] H. F. Grip, L. Imsland, T. A. Johansen, I. Fossen, J. C. Kalkkuhl and A. Suissa, Nonlinear vehicle side-slip estimation with friction adaptation. Automatica, Vol. 44, No. 3, 2008, pp. 611622.
- [7] D. Selmanaj, M. Corno, G. Panzani and S.M. Savaresi, Vehicle sideslip estimation: A kinematic based approach. Control Engineering Practice, Vol. 67, October 2017, pp. 1-12.
- [8] J. Farrelly and P. Wellstead, Estimation of vehicle lateral velocity. Proceedings of the 1996 IEEE International Conference on Control Applications, 1996, pp. 552557.
- [9] H. F. Grip, L. Imsland, T. A. Johansen, J. C. Kalkkuhl and A. Suissa, Vehicle sideslip estimation. IEEE Control Systems, Vol. 29, No. 5, October 2009, pp. 36-52.
- [10] B. Heißing and M. Ersoy, Chassis handbook: fundamentals, driving dynamics, components, mechatronics, perspectives. Springer Science & Business Media, 2010.